https://ntrs.nasa.gov/search.jsp?R=19810068617 2020-03-21T10:59:20+00:00Z

NATIONAL ADVISORY COMMITTEE FOR AERONAUTICS

TECHNICAL NOTE

No. 1691

ICING AND DE-ICING OF A PROPELLER WITH INTERNAL ELECTRIC BLADE HEATERS

By James P. Lewis and Howard C. Stevens, Jr.

Flight Propulsion Research Laboratory
Cleveland, Ohio

Washington
August 1948

NATIONAL ADVISORY COMMITTEE FOR AERONAUTICS

TECHNICAL NOTE NO. 1691

ICING AND DE-ICING OF A PROPELLER WITH INTERNAL ELECTRIC BLADE HEATERS

By James P. Lewis and Howard C. Stevens, Jr.

SUMMARY

An investigation has been made in the NACA Cleveland icing research tunnel to determine the de-icing effectiveness of an experimental configuration of an internal electric propeller-blade heater. Two atmospheric icing conditions and two propeller operating conditions were investigated in experiments with unheated blades and with heat applied to the blades both continuously and cyclically. Data are presented to show the effect of propeller speed, ambient-air temperature and liquid-water concentration, and the duration of the heat-on and cycle times on the power requirements and de-icing performance of the blade heaters.

The extent of ice-covered area on the blades for various icing and operating conditions has been determined. The largest iced area was obtained at the higher ambient-air temperatures and at low propeller speed. The chordwise extent of icing in practically every case was greater than that covered by blade heaters.

Adequate de-icing in the heated area with continuous application of heat was obtained with the power available but a maximum power input of 1250 watts per blade was insufficient for cyclic de-icing for the range of conditions investigated. Blade-surface temperature rates of rise of 0.2° to 0.7° F per second were obtained and the minimum cooling period for cyclic de-icing was found to be approximately $2\frac{1}{2}$ times the heating period.

INTRODUCTION

Several methods of obtaining icing protection for propellers have been proposed including the use of alcohol or other freezing-point depressants, the external electric blade heaters (reference 1), and the passage of a hot gas through a hollow blade (reference 2).

The recent development of hollow steel propeller blades constructed with a thin sheet-metal outer skin has permitted the installation of an electric heater within the blade. Such a heater installation does not impair the aerodynamic performance of the blade and is free from abrasion damage. Theoretical analysis (reference 3) and flight investigations (reference 4) of heat requirements for ice prevention with continuous heating have indicated that the electric power needed is excessive for current aircraft. An investigation concerned with both continuous and cyclic heating systems was therefore conducted at the NACA Cleveland laboratory to determine the icing protection provided by an experimental configuration of an internal electric propeller-blade heater and the effects of several icing, heating, and propeller operating conditions on the heater performance.

The investigation was made under simulated icing conditions in the NACA Cleveland icing research tunnel. Two propeller operating conditions and two icing conditions were investigated, together with several power inputs and heat-on and cycle times. Data are presented to show the effect of propeller speed, ambient-air temperature and liquid-water concentration, heating power input, and the duration of the heat-on and heat-off times on the blade-heater power requirements and performance.

APPARATUS AND INSTRUMENTATION

The propeller on which the investigation was conducted was mounted on a modified airplane fuselage located in the diffuser section of the icing research tunnel. The location of the installation and of the water sprays, together with details of the setup, are shown in figure 1(a); a photograph of the propeller installation is shown in figure 1(b). The experimental propeller was a 15-foot, four-blade, hollow, steel propeller reduced to an 11-foot diameter to permit installation in the tunnel. The blade construction consisted of a tubular main spar to which steel sheets of 0.037-inch thickness were attached to form the blade profile, an NACA 16-series airfoil section. A semihard sponge rubber within the forward blade cavity served as a vibration dampener. The blade-form characteristics (thickness-chord ratio h/b, chord-diameter ratio b/D, leading-edge-chord radius ratio r_{LE}/b, blade angle β, and design-lift coefficient C_L) are given in figure 2. Electric power for the blade heaters installed in each of the four blades was supplied through autotransformers

and an electronic timer and was conducted to the blades by a slip-ring assembly mounted at the rear of the propeller hub. Details of the power-supply system are given in reference 1.

Propeller-blade heaters. - The blade heater consisted of a varied distribution of electric resistance wires sewed between two layers of nylon fabric, cemented to the inner surface of the leading-edge cavity, and held in place by the sponge filler. Details of the heater construction and installation including the metallic leading-edge fillet are given in figure 3. The heated area extended from the leading edge to approximately 20 percent of chord on both the thrust and and camber faces. The heating element was 47 inches long and extended inboard from the blade tip to approximately 4 inches from the shank end of the blade. The total heated area per blade was approximately 200 square inches. The power density at the inner surface was approximately twice as great at the leading edge as at the rear of the heaters. The design power-density distribution on the inner surface of the blade for a power input of 1000 watts per blade at five radial stations is shown in figure 4. These curves were obtained from Hamilton-Standard Propellers Division, United Aircraft Corporation. Temperature limitations of the nylon and the sponge rubber restricted the safe power input to 1250 watts per blade.

Instrumentation. - Instrumentation was provided to measure the propeller speed, ambient-air temperature, power to the heating elements, heat-on and cycle times, tunnel airspeed, and blade-surface temperatures.

The propeller speed was measured by a standard aircraft tachometer with an accuracy of ±3 percent. The ambient-air temperature was measured by two thermocouples mounted on the tunnel turning vanes at each side of the setup and approximately 15 feet downstream of the propeller. The accuracy of the ambient-air temperature measurements was approximately ±3° F. Blade-surface temperatures were measured by temperature-sensitive electric resistance gages, which were similar to strain gages. A total of 40 gages were installed on two adjacent blades. A full description of the surface-temperature-measuring system is given in reference 1. A shift in the calibration of the blade-surface-temperature galvanometer necessitated the application of a correction to the indicated surface temperature. A correction was obtained by taking the difference between the indicated blade-surface temperature and the sum of the tunnel ambient-air temperature and the local kinetic temperature rise. This correction was computed for each gage and each experiment for the dry unheated condition and was then subtracted from the subsequent indicated temperatures obtained for each experiment during icing and heating.

Observations and photographs of the propeller in operation were made using a stroboscopic lighting system consisting of four flash lamps synchronized with the propeller.

Water-spray system. - Icing conditions were simulated by spraying water into the refrigerated tunnel air stream. A group of 46 air-atomizing nozzles, enclosed in a steam-heated fairing and located around the periphery of the tunnel immediately ahead of the contraction section (fig. 1(a)), discharged the spray water perpendicularly to the air stream. The icing conditions in the tunnel were determined by the method described in reference 1.

CONDITIONS AND PROCEDURE

Data were obtained for a series of icing and de-icing conditions each of which was of 10- to 15-minute duration. Propeller speed, ambient-air temperature, and airspeed were maintained constant and recorded at 1-minute intervals. Propeller-blade-surface temperatures were recorded either continuously or intermittently. Photographs were made during operation using the stroboscopic-flash-lamp system. Visual observations of icing and de-icing were made during operation and photographs and sketches were made immediately after each stop.

Operating conditions. - A tunnel airspeed of 120 miles per hour was held constant throughout the investigation. This velocity was the average at the 42-inch-radius station of the propeller as determined by a velocity survey of the tunnel (reference 1). The propeller was operated at speeds of 800 and 1000 rpm with blade angles of 34.5° and 30.5°, respectively. These propeller speeds correspond to advance diameter ratios of 1.2 and 0.96, respectively, and were chosen as being representative of low-speed and cruising conditions, respectively. Because of the nature of the tunnel velocity distribution, the shank end of the blades operated at small negative angles of attack; hence, the area of water interception extended further aft on the camber face at this region.

Icing conditions. - The investigation was conducted at two icing conditions that were defined by the ambient-air temperature, liquid-water concentration, and droplet diameter. The conditions used were at average ambient-air temperatures of 3° and 18° F with corresponding liquid-water concentrations of 0.3 and 0.7 gram per cubic meter. An average droplet diameter of 55 microns, as determined by the volume maximum, was found but no consistent variation with temperature was obtained. The method of calibrating the

water sprays and the applicability of the results obtained are discussed in reference 1. The variation of the average liquid-water concentration with ambient-air temperature is shown in figure 5(a) and the radial variation of water concentration is shown in figure 5(b). The values of liquid-water concentration recommended at the Mount Washington Observatory-Weather Bureau meeting of June 1945 and an envelope of values from numerous ground and flight observations as reported by the Army Air Forces in 1946 are also shown in figure 5(a). Subsequent information given in reference 5 shows some values of liquid-water concentration found in cumulus clouds in excess of those shown on the curve. The marked decrease in liquid-water concentration in the tunnel with decreasing ambient-air temperatures (fig. 5(a)) for a constant input of spray water indicates that the amount of frozen-water particles increased with decreasing temperature.

Blade-heating conditions. - Power inputs of 500, 750, 1000, and 1250 watts per blade were used either continuously or cyclically in the de-icing investigation. The heat-on and the cycle times investigated were as follows:

Heat-on time (sec)	Heat-off time (sec)	Total cycle time (sec)	Cycle ratio
5	15	20	1:4
5	35	40	1:8
10	10	20	1:2
10	30	40	1:4
10	70	80	1:8
20	60	80	1:4
20	140	160	1:8
30	90	120	1:4
30	210	240	1:8
40	40	80	1:2
40	120	160	1:4
50	150	200	1:4

The cycle ratio is defined as the ratio of the heat-on time to the total cycle time. All the heating cycles listed were not investigated at all the power levels and operating conditions. Two different power inputs or two de-icing cycles were used successively in several of the experiments. In many cases heat was supplied to only one pair of diametrically opposite blades in order that a comparison between heated and unheated blades would clearly show the relative de-icing effectiveness of the heater installation in the same icing conditions.

RESULTS AND DISCUSSION

The results of the investigation are discussed with respect to the ice formations on unheated blades, continuous heating, and cyclic de-icing.

Ice formations on unheated blades. - Views of typical ice formations on the unheated blades are shown in figure 6. The blades are shown with the shank towards the bottom and the leading edge at the center. At a propeller speed of 800 rpm, ambient-air temperature of 17° F, a liquid-water concentration of 0.7 gram per cubic meter, and a blade angle of 34.5° (fig. 6(a)), a rough irregular rime-ice formation, which extended the full length of the blade on the leading edge, was obtained. On the camber face the ice extended to 100 percent of chord from the shank to approximately 60 percent of the radius and then diminished to the leading edge at the tip. On the thrust face practically the entire outer 50 percent of the blade was covered. The negative angles of attack caused by the nonuniform tunnel-velocity distribution at the inner end of the blade were responsible for the lack of ice in this region. At a propeller speed of 800 rpm, an ambient-air temperature of 17° F, a liquid-water concentration of 0.7 gram per cubic meter, a blade angle of 30.5°, similar formations to those at a blade angle of 34.5° were obtained on the camber face (fig. 6(a)). Very little ice was obtained on the thrust face because of the decrease in blade angle. Lowering the ambient-air temperature to 2° F resulted in a very small formation of smooth fine rime ice (fig. 6(a)). As at the temperature of 17° F, very little icing occurred on the thrust face.

At a propeller speed of 1000 rpm (fig. 6(b)), the ice formations were similar to those obtained at 800 rpm at corresponding ambient-air temperatures and blade angles. Both the chordwise and the radial extent of icing were less than at 800 rpm. At an ambient-air temperature of 17° F and a blade angle of 30.5°, a rough irregular rime formation extended to approximately 80 percent of radius. Light formations on the thrust face were confined to the center portion of the blade. At an ambient-air temperature of 22° F and a blade angle of 34.5°, the ice formation on the leading edge extended to approximately 90 percent of radius and there was indication of runback particularly on the inner portion of the thrust face.

The radial extent of the ice formations on unheated blades for the conditions investigated varied from 50 to 100 percent of the blade radius. A chordwise coverage on the camber face as

great as 100 percent of chord at the shank end was obtained with the formations gradually tapering toward the leading edge in a radial direction. On the thrust face a chordwise coverage of 100 percent was obtained at the blade tip. The largest formations were obtained at the higher ambient-air temperatures and low propeller speed. The smallest formations were obtained at the lowest ambient-air temperature and low propeller speed and blade angle. With the exception of the formations at the lowest ambient-air temperature, a rough irregular formation,which showed evidence of natural shedding, was obtained.

The nonuniform nature of the velocity distribution in the tunnel was such as to change the local blade angle of attack, thus causing the position of the ice formation to be different from that obtained in natural icing conditions. As a result, an ice coverage of 100 percent of chord was obtained at the shank end on the camber face and at the tip on the thrust face. In addition, the large droplet size (55 microns) increased the chordwise extent of icing on the camber face over that obtained in natural icing conditions. Within the radial extent of icing, the chordwise coverage in practically every case extended beyond the rear margin of the blade heaters (20 percent of chord).

Continuous heating. - The results of continuous heating of the blades are summarized in table I. The results are given in terms of the percentage de-icing effectiveness, which was defined as the ratio of the percentage of heater area cleared of ice by heating to the percentage of heater area iced with no heat to the blades. The area cleared by heating was taken as the difference between the iced areas with and without heat. The heater area was used as a basis for effectiveness because the heaters were ineffective in removing ice beyond the area immediately surrounding them. This method of rating, therefore, does not consider runback and refreezing aft of the rear margin of the heaters. Heating of the blades was continued for a period of time long enough to allow the blade temperatures to reach a stable value and until no further improvement in ice removal was observed.

With continuous heating of the blades at a propeller speed of 1000 rpm and an ambient-air temperature of 18° F (condition A, table I), a de-icing effectiveness of 100 and 95 percent on the thrust and camber faces, respectively, was obtained with a power input of 500 watts per blade (average power density, 2.5 watts/sq in.) and 100-percent effectiveness on both faces was obtained at a power input of 750 watts per blade (average power density, 3.75 watts/sq in.; condition B).

The effect of ambient-air temperature is indicated by the requirement, at 1000 rpm and 1° F (condition D), of 1000 watts per blade (average power density, 5 watts/sq in.) for 100-percent effectiveness.

When the propeller speed was lowered to 800 rpm at an ambient-air temperature of 18° F (condition C), a power input of 1000 watts per blade resulted in 100-percent effectiveness. At a propeller speed of 800 rpm and an ambient-air temperature of 4° F (condition E), de-icing effectiveness of 90 and 85 percent for the thrust and camber faces, respectively, were obtained at 1000 watts per blade. An increase of the power input to 1250 watts per blade (average power density, 6.25 watts/sq in.) resulted in 100-percent effectiveness on both the thrust and camber faces (condition F).

The typical rise of blade-surface temperatures above ambient-air temperature during icing with continuous heating is shown in figure 7. The rise of the leading-edge surface temperatures at the 33-percent radius, ambient-air temperatures of 1° and 4° F, and propeller speeds of 800 and 1000 rpm, respectively, for a power input of 1000 watts per blade is shown in figure 7(a). The temperature rise for an unheated blade at 800 rpm is also shown. The temperatures for propeller speeds of both 800 and 1000 rpm had an initial rate of rise for the first 30 seconds of heating of approximately 0.6° F per second, which gradually decreased until a stable value was reached. At a propeller speed of 800 rpm, a stable value of approximately 67° F above ambient-air temperature was attained after about 240 seconds of heating. At a propeller speed of 1000 rpm, a value of approximately 54° F above ambient-air temperature was reached in a heat-on time of about 150 seconds.

The rise of the blade-surface temperatures at a point 2 inches from the leading edge on the camber face at 33-percent radius for the same speed and power conditions and one additional condition is shown in figure 7(b). At ambient-air temperatures of 1° and 4° F, the average rate of rise in the first 30 seconds of heating for both 800 and 1000 rpm was approximately 0.5° F per second. A peak stable value of 39° F above ambient-air temperature at 800 rpm and an ambient-air temperature of 4° F was reached in approximately 180 seconds and a value of 37° F above ambient-air temperature at 1000 rpm was reached in approximately 150 seconds. At an ambient-air temperature of 18° F and a propeller speed of 800 rpm, the initial rate of rise was considerably lower (0.2° F/sec) and a peak value of 23° F above ambient-air temperature was obtained in approximately 90 seconds. The difference in blade temperature rise

at the different ambient-air temperatures may be attributed mainly to the formation of ice and subsequent release of heat at the lower ambient-air temperatures, which was not apparent at the higher ambient-air temperature. The differences in blade temperatures at the leading edge and 2 inches from the leading edge are primarly due to differences in the local power density. The power density on the inner surface at the leading edge was approximately $6\frac{1}{2}$ watts per square inch, whereas at 2 inches from the leading edge it was 3 watts per square inch (fig. 4).

Views of typical residual ice formations after continuous heating are shown in figure 8. Notice should be made of the rather large ice formations at the shank end of the blades. An area at the shank approximately 4 inches long was unheated and the ice formations at this region were extremely difficult to remove. Ice in the heated area was also attached to this unheated area, thus increasing the difficulty of ice removal. At a propeller speed of 800 rpm, ambient-air temperature of 18° F, liquid-water concentration of 0.7 gram per cubic meter, blade angle of 30.5°, and power input of 1000 watts per blade, indications of runback and refreezing are evident. Practically no de-icing behind the heated area was obtained.

A series of stroboscopic photographs taken during icing and de-icing are shown in figure 9. These photographs were made with condition C: propeller speed of 800 rpm, an ambient-air temperature of 18° F, and a blade angle of 30.5° with a power input of 1000 watts per blade being applied after 7 minutes of icing. De-icing started following the applications of heat and the heated area was almost completely cleared of ice within 5 minutes with very little change in de-icing thereafter.

Cyclic heating. - The results of the investigation of cyclic heating are presented in terms of de-icing effectiveness in table II. In general, less satisfactory performance was obtained with cyclic than with continuous application of heat. Because of limitations of the heater power input (1250 watts/blade maximum), the requirements for 100-percent effectiveness could not be determined for the range of heat-on times investigated. At ambient-air temperatures of 17° to 20° F and a propeller speed of 1000 rpm, the best de-icing effectiveness observed was 90 and 95 percent on the thrust and camber faces, respectively, at heat-on time of 30 seconds, total cycle time of 120 seconds, and power input of 1000 watts per blade (condition K). Decreasing the propeller speed to 800 rpm at approximately the same icing and heating condition (condition Q)

decreased the effectiveness to 85 and 90 percent. Although less ice formed on the blade at 800 rpm than at 1000 rpm, the decrease in de-icing effectiveness may be due to the difference in centrifugal force. Lowering the ambient-air temperature from 17° to 3° F (condition S) decreased the effectiveness to 5 and 10 percent.

The effect of increasing power input particularly at low temperatures is shown by the increase in effectiveness from 20 percent on both faces (condition T) to 60 and 70 percent on the thrust and camber faces, respectively, (condition U) when the power was changed from 1000 to 1250 watts per blade. At higher temperatures of 17° and 20° F and a shorter cycle (conditions M and N), the effectiveness increased from 70 and 75 percent to 80 and 90 percent.

The effect of increasing the heat-on time from 10 to 24 seconds at an approximately constant cycle time is shown by the increase in effectiveness from 70 percent on both faces to 80 percent on the thrust face and 90 percent on the camber face (conditions L and N) when the heat-on time was increased. The de-icing effectiveness was decreased from 85 and 80 percent on the thrust and camber faces, respectively, to 65 percent when the cycle time was increased from 120 to 240 seconds at a constant heat-on time, (conditions P and O). The effect of varying the heat-on time can be seen by comparing conditions B, I, and K where, for a constant cycle ratio of 1:4, increasing the heat-on time from 5 to 30 seconds gave improved de-icing effectiveness. For each icing, heating, and operating condition the best results were obtained with the longest heat-on time (30 to 50 sec).

In general, the best results with cyclic heating were obtained with a cycle time approximately four times the length of the heat-on time. Cycle ratios as low as 1:2 gave more effective de-icing than the 1:4 ratio only at the highest power input and longer heat-on times.

Typical variations of blade-surface temperatures with time during cyclic de-icing for various icing, heating, and operating conditions are given in figure 10. Results are shown for the temperatures of the leading edge at 33-percent radius. The blade-temperature variation at propeller speed of 1000 rpm, heat-on time of 20 seconds, cycle time of 80 seconds, and power input of 750 watts per blade, is shown in figure 10(a) (condition C). The temperature rose approximately 13° F when the water sprays were turned on and reached 33° F before the application of heat. Blade heat-on times of 20 seconds resulted in an average rise of approximately 4° F after the start of cyclic heating. The blade temperatures decreased quickly when heating stopped and returned to the freezing point.

The blade temperatures for the heat-on time of 20 seconds and the cycle time of 80 seconds at propeller speed of 800 rpm, two ambient-air temperatures, and power input of 1000 watts per blade are shown in figures 10(b) and 10(c) (conditions M and R, respectively). The results at the higher temperature (17° F) (fig. 10(b)) are much the same as obtained at the 750-watt power input (fig. 10(a)). The blade temperatures again remained above 32° F. At a lower ambient-air temperature of -1° F, (fig. 10(c)), greater temperature rises were obtained and for most cycles the heated-blade temperatures returned to the unheated-blade temperature. The power input and heat-on times were insufficient to raise the blade temperature above freezing and practically no de-icing was obtained anywhere on the blade.

The effect of longer heat-on and cycle times at the same heating and operating conditions is shown in figures 10(d) and 10(e) (conditions S and Q, respectively). Larger temperature rises were obtained with the temperature remaining above 32° F for a period sufficient to accomplish de-icing. As shown in figure 10(d), the heated blade cooled almost to the unheated-blade temperature when heating stopped. The effect of further increases in heat-on and cycle times is shown in figures 10(f) and 10(g) for conditions U and W, respectively.

The blade temperatures obtained at a propeller speed of 800 rpm and a power input of 1250 watts per blade are shown in figures 10(h) and 10(i). At an ambient-air temperature of 5° F, a heat-on time of 40 seconds, and a cycle time of 80 seconds, average peak temperatures of 37° F were obtained (fig. 10(h), condition V). At an ambient-air temperature of 20° F, a heat-on time of 24 seconds, and a cycle time of 84 seconds, the initial blade rise caused by the water sprays raised the blade temperature to freezing (fig. 10(i), condition N). The blade temperatures remained above freezing during the subsequent heating cycles with a minimum value of 37° F resulting. The temperature curves indicate too short a cooling period and too much power input.

Views of the residual ice formations on the blades after cyclic de-icing are shown in figure 11. The percentage of de-icing effectiveness obtained for each condition is given in table II. The photographs show the difficulty in removing ice from the unheated area at the shank of the blades and the ineffectiveness of the heater in removing ice in the region behind the heated area. Comparison of figure 11 with figure 8, shows that no significant difference was obtained in runback and refreezing between continuous

and cyclic heating. The only significant runback was obtained at ambient-air temperatures of 20° F and above (fig. 11(a), 11(c) and 11(d)). The residual formations for the low-temperature conditions (fig. 11(b)) show ineffective de-icing obtained at low ambient-air temperatures. The ice formation on the blades is practically the same as that obtained with the unheated blade (fig. 6(a)).

At a power input of 1000 watts per blade, the blade temperature rate of rise varied from 0.7° F per second at an ambient-air temperature of 3° F to 0.2° F per second at an ambient-air temperature of 17.5° F. At a power input of 1250 watts per blade, the rate of rise varied from 0.7° F per second at ambient-air temperature of 5° F per second at an ambient-air temperature 20° F. An average rate of rise of 0.6° F per second was obtained.

The variation in the length of the optimum cooling period with the heating period is shown in figure 12. No significant variation with power input was found for the icing, heating, and operating conditions investigated. The cooling periods shown in figure 12 were the minimum periods in which complete cooling to the temperature at the start of the heating cycle was attained. The average minimum cooling period was found to be approximately $2\frac{1}{2}$ times the heat-on time.

SUMMARY OF RESULTS

The following results were obtained from an ice-tunnel investigation of an internally heated propeller blade at propeller speeds of 800 and 1000 rpm, ambient-air temperatures from -1° to 20° F, liquid-water concentrations from 0.3 to 0.9 gram per cubic meter, heat-on time from 5 to 54 seconds, cycle time from 30 to 240 seconds, blade angles of 30.5° and 34.5°, and power inputs from 750 to 1250 watts per blade:

1. For the conditions investigated, the ice formations on unheated blades varied from 50 to 100 percent of the blade radius. A chordwise coverage on the camber face as great as 100 percent of the chord at the shank end of the blade was obtained with the formation tapering toward the leading edge at the tip. On the thrust face a chordwise coverage of 100 percent was obtained at the blade tip. The largest formations were obtained at the higher ambient-air temperatures and at the low propeller speed. The smallest formations were obtained at the lowest ambient-air temperature and at the low propeller speed and blade angle. Within the radial

extent of icing, the chordwise coverage of icing in practically every case extended beyond the rear margin of the blade heaters.

2. With continuous heating, 100-percent de-icing effectiveness for the heated area was obtained at 18° F with a power input of 750 watts per blade. At an ambient-air temperature of 1° F, 1000 watts per blade were required for 100-percent de-icing at 1000 rpm but lowering the propeller speed to 800 rpm and raising the power input to 1250 watts per blade resulted in approximately 100-percent average effectiveness. Stable maximum temperatures with continuous heating were obtained within periods of approximately 90 to 240 seconds.

3. De-icing effectiveness with cyclic heating was considerably less than for continuous heating of the blades. The best de-icing (90 to 95 percent) with cyclic heating was obtained at heat-on time of 30 seconds, total cycle time of 120 seconds, and power input of 1000 watts per blade, for the conditions of propeller speed of 1000 rpm and ambient-air temperature of 17° to 19° F. The best de-icing for the conditions investigated required heat-on times of 30 to 50 seconds. No significant difference was obtained in run-back and refreezing between continuous and cyclic heating.

4. For ambient-air temperatures of 0° to 17° F it is estimated that power inputs of approximately 1500 watts per blade, a heat-on time of approximately 60 seconds, and a total cycle time of approximately 240 seconds would be required for adequate de-icing. (These values apply only to propellers similar to that investigated.) No conclusions can be made as to the optimum power distribution as the experimental heater had a fixed power distribution.

5. The effectiveness of the blade sponge filler as a thermal insulation was indicated by the small amount of de-icing obtained in the area behind the heater.

6. Blade-temperature rates of rise of 0.2° to 0.7° F per second were obtained with the rate of rise a function of ambient-air temperature. A required minimum cooling period of approximately $2\frac{1}{2}$ times the heating period was found.

CONCLUSIONS

From the results of this investigation, several significant conclusions can be drawn concerning the requirements for the design

and operation of internal electric propeller-blade heaters. Due consideration must be given to the difference between the simulated and natural icing conditions and to the special construction of the experimental heating element.

1. Despite the marginal performance of the experimental installation, cyclic de-icing with an internal electric blade heater appears to be a practicable method of propeller ice protection.

2. The chordwise extent of heating on the propeller was inadequate for the icing conditions to which the propeller was subjected; minimum extent of chordwise heating cannot be exactly specified in the absence of data concerning the effects of residual ice formations on propeller performance. Because the results show that the radial extent of icing varies widely with changes in propeller speed and icing conditions, the radial extent of heating will be dependent on the particular design conditions and the tolerable extent of icing on propeller performance. Unheated areas at the shank of the blade seriously impair de-icing and should be eliminated.

Flight Propulsion Research Laboratory,
National Advisory Committee for Aeronautics,
Cleveland, Ohio, February 4, 1948.

REFERENCES

1. Lewis, James P.: De-Icing Effectiveness of External Electric Heaters for Propeller Blades. NACA TN No. 1520, 1947.

2. Mulholland, Donald R., and Perkins, Porter J.: Investigation of Effectiveness of Air-Heating a Hollow Steel Propeller for Protection Against Icing. Part I - Unpartitioned Blades NACA TN No. 1586, 1948.

3. Scherrer, Richard: An Analytical Investigation of Thermal-Electric Means of Preventing Ice Formations on a Propeller Blade. NACA ACR No. 4H31, 1944.

4. Scherrer, Richard, and Rodert, Lewis A.: Tests of Thermal-Electric De-Icing Equipment for Propellers. NACA ARR No. 4A20, 1944.

5. Lewis, William: A Flight Investigation of the Meteorological Conditions Conducive to the Formation of Ice on Airplanes. NACA TN No. 1393, 1947.

TABLE I - RESULTS OF CONTINUOUS-HEATING INVESTIGATION

Condition	Propeller speed (rpm)	Average ambient-air temperature (°F)	Average liquid-water concentration (gram/cu m)	Heat-on time (min)	Blade angle at 42-inch radius (deg)	Heater power input (watts/blade)	De-icing effectiveness (percent)		Figure
							Thrust face	Camber face	
A	1000	18	0.7	$10\frac{1}{2}$	30.5	500	100	95	------
B	1000	18	.7	5	30.5	750	100	100	------
C	800	18	.7	8	30.5	1000	100	100	7(b), 8, 9
D	1000	1	.2	9	30.5	1000	100	100	7(a), 7(b), 8
E	800	4	.2	$3\frac{1}{2}$	34.5	1000	90	85	7(a), 7(b), 8
F	800	4	.2	6	34.5	1250	100	100	8

TABLE II - RESULTS OF CYCLIC DE-ICING INVESTIGATION

Condition	Propeller speed (rpm)	Average ambient-air temperature (°F)	Average liquid-water concentration (gram/cu m)	Heat-on time (sec)	Cycle time (sec)	Blade angle at 42-inch radius (deg)	Heater power input (watts/blade)	De-icing effectiveness (percent)		Figure
								Thrust face	Camber face	
A	1000	17	0.7	5	40	30.5	1000	10	10	----------
B		17	.7	5	20		1000	50	30	11(e)
C		19	.9	20	80		750	10	15	10(a)
D		17	.7	10	40		750	50	40	----------
E		17	.6	10	20		750	------	50	----------
F		18	.7	10	20		1000	80	80	----------
G		20	.8	20	160		750	60	60	11(d)
H		17	.7	20	80		750	40	55	11(d)
I		18	.7	20	80		1000	85	85	11(e)
J		20	.8	30	240		750	85	80	----------
K		19	.8	30	120		1000	90	95	----------
L	800	20	0.8	10	80	34.5	1250	70	70	----------
M		17	.7	20	80		1000	70	75	11(b), 10(b)
N		20	.8	24	84		1250	80	90	11(c), 10(i)
O		20	.8	30	240		750	65	65	11 11(a)
P		21	.9	30	120		750	85	80	11(a)
Q		17	.7	34	124		1000	85	90	10(e)
R		-1	.3	20	80		1000	15	10	11(b), 10(c)
S		3	.3	32	120		1000	5	10	10(d)
T		5	.3	40	160		1000	20	20	----------
U		5	.4	44	160		1000	60	70	10(f)
V		5	.3	40	80		1250	90	80	11(c), 10(h)
W		4	.3	54	196		1000	40	50	10(g)

NACA

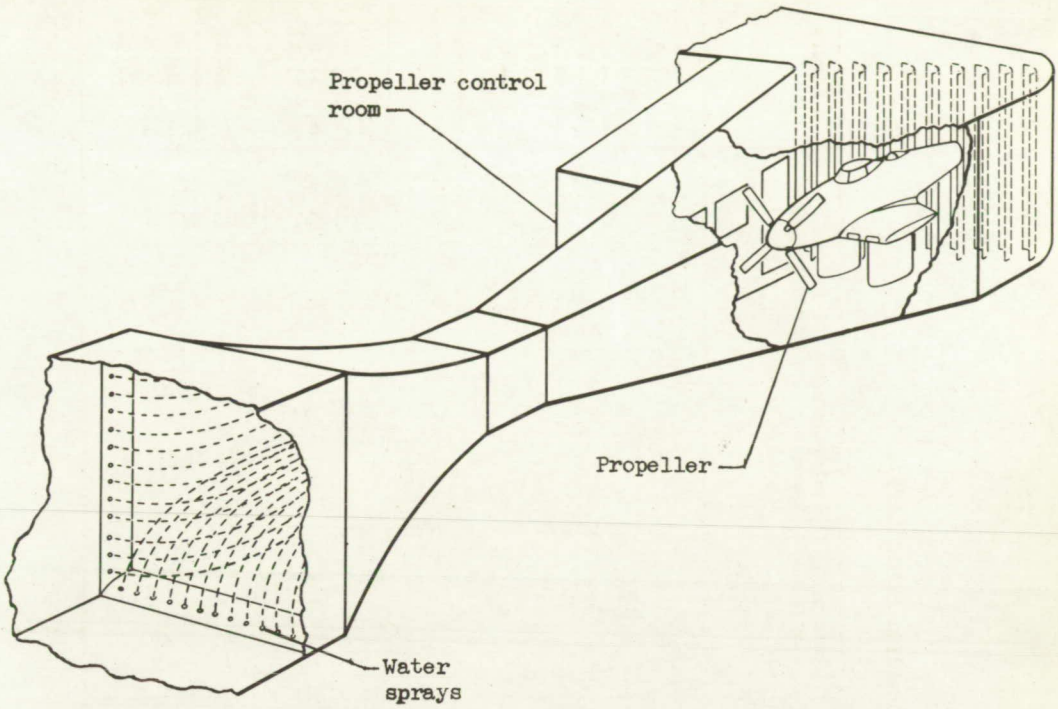

(a) Location of setup in icing research tunnel.

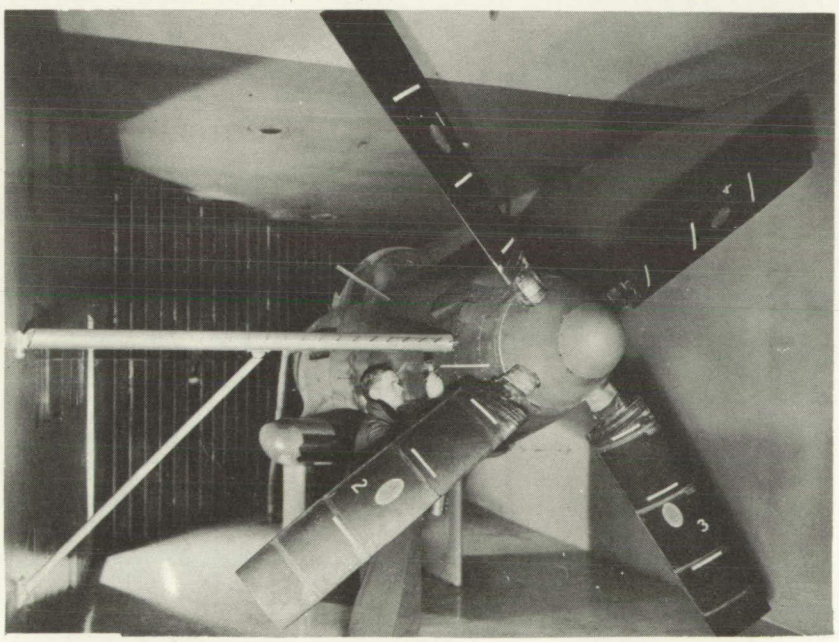

NACA
C-13823
12-7-45

(b) Propeller mounted in icing research tunnel.

Figure 1. - Propeller-icing research installation.

Page intentionally left blank

Page intentionally left blank

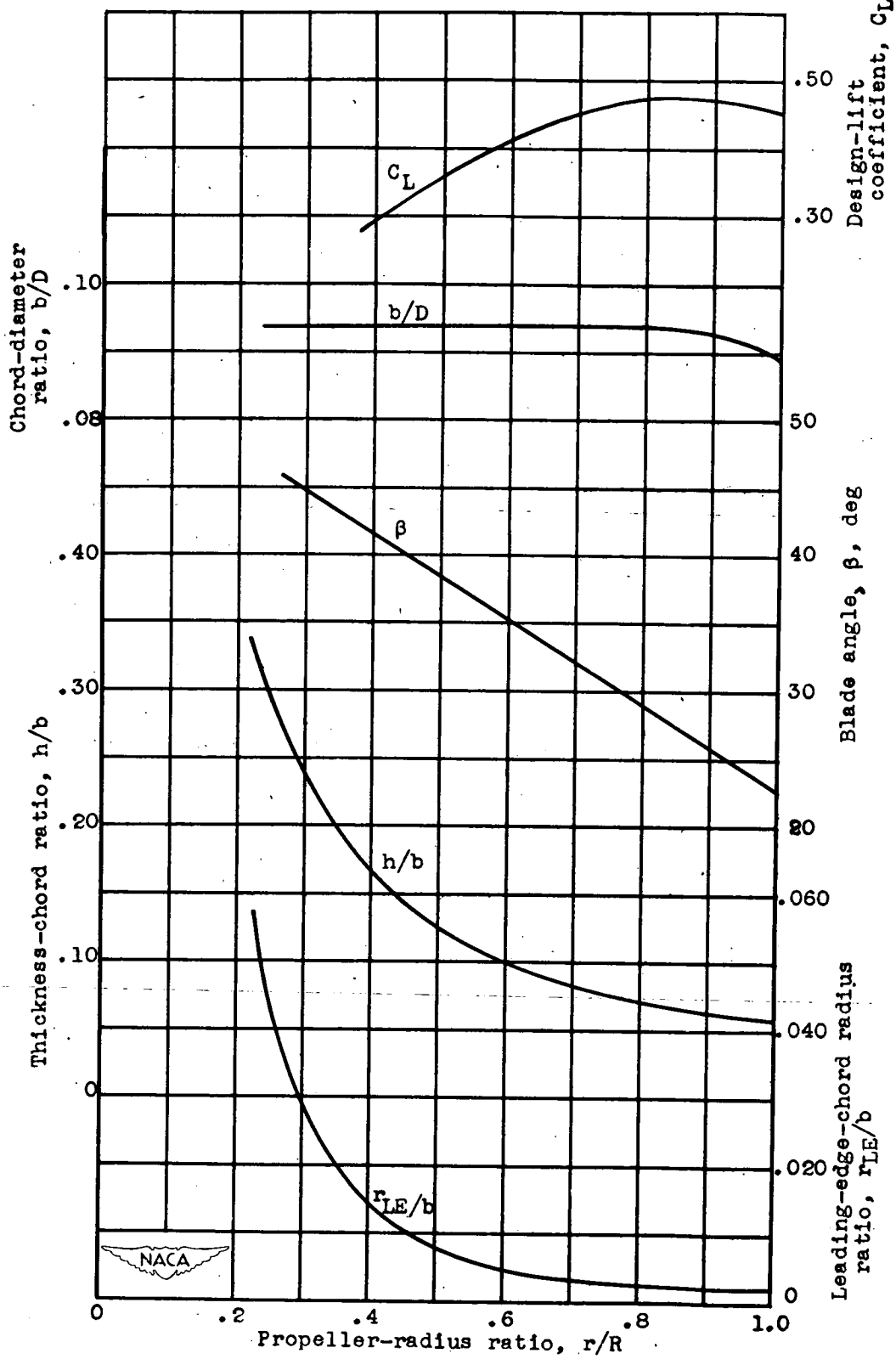

Figure 2.- Blade-form characteristics for propeller blade with internal blade heater.

Page intentionally left blank

Page intentionally left blank

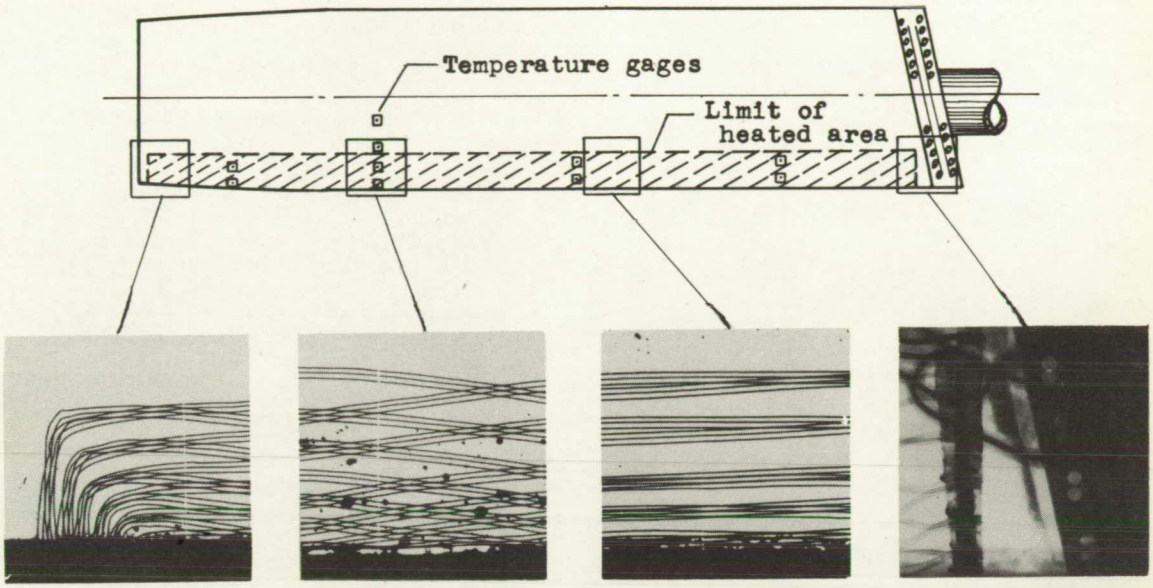

(a) Plan form of blade and sectional X-ray views.

NACA
C-20533
1-29-48

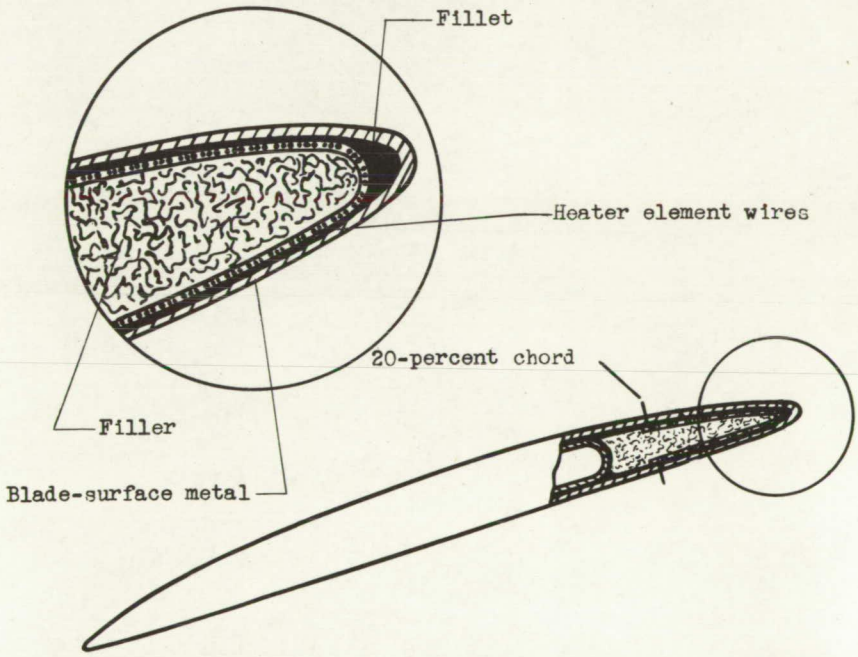

(b) Cross section of heater at propeller-radius ratio of 0.75.

Figure 3. - Details of heater construction.

Page intentionally left blank

Page intentionally left blank

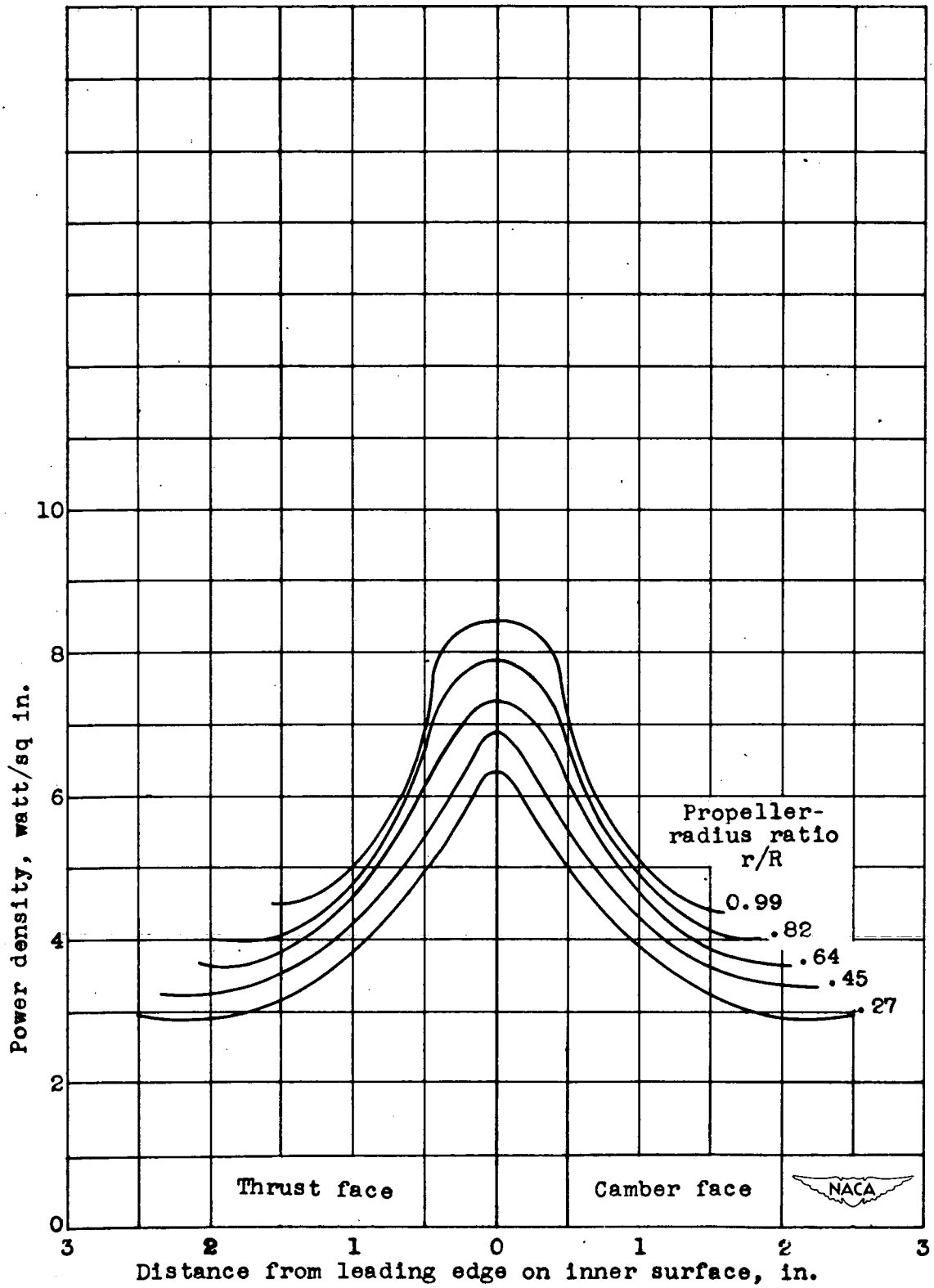

Figure 4.- Design power distribution at 1000 watts per blade (taken from data supplied by manufacturer).

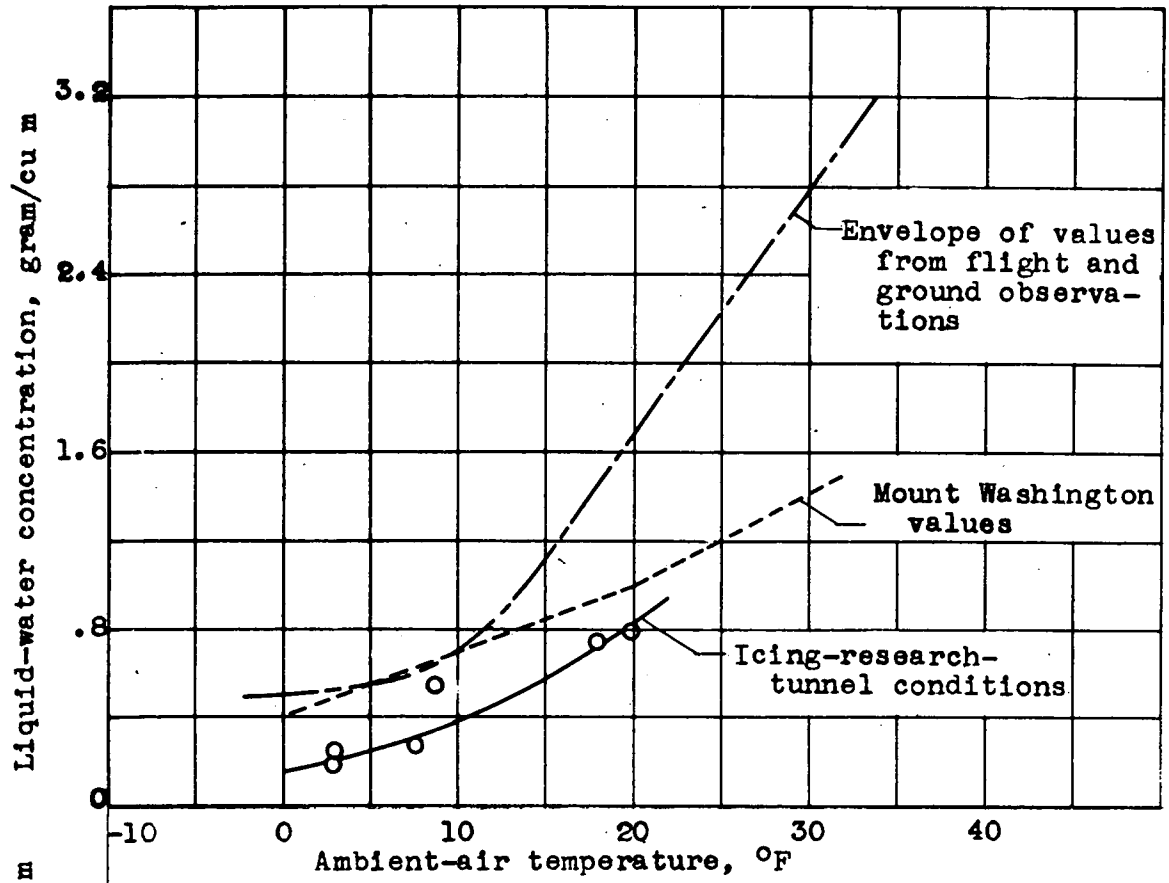

(a) Variation of liquid-water concentration with air temperature.

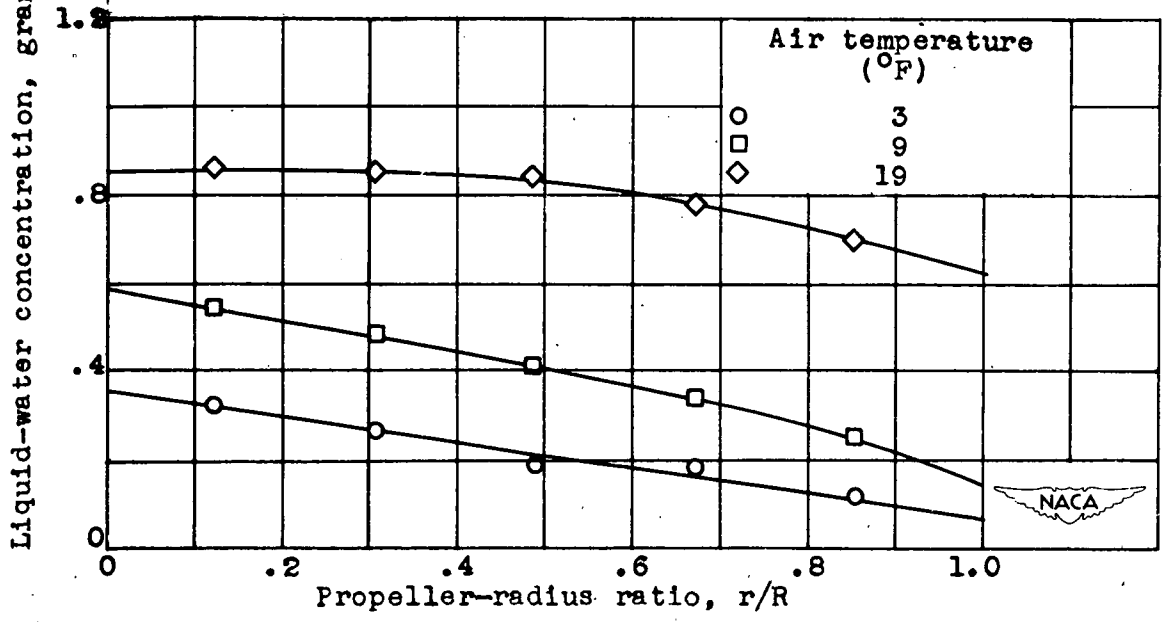

(b) Radial distribution of liquid-water concentration.

Figure 5.- Icing conditions for propeller-icing research.

	Thrust Camber	Thrust Camber	Thrust Camber
Ambient-air temperature, °F	17	17	2
Liquid-water concentration, gram/cu m	0.7	0.7	0.2
Blade angle, deg	34.5	30.5	30.5

NACA
C-20535
1-29-48

(a) Propeller speed, 800 rpm.

Figure 6. - Ice formations obtained at various icing and operating conditions with unheated blades.

Page intentionally left blank

Page intentionally left blank

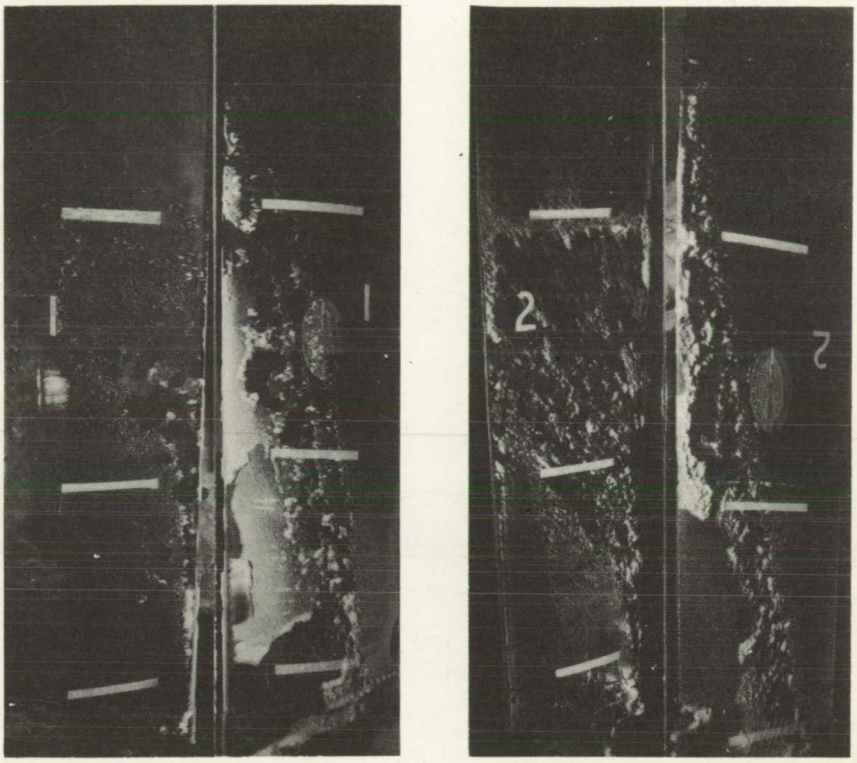

	Thrust Camber	Thrust Camber
Ambient-air temperature, °F	17	22
Liquid-water concentration, gram/cu m	0.7	0.9
Blade angle, deg	30.5	34.5

NACA
C-20534
1-29-48

(b) Propeller speed, 1000 rpm.

Figure 6. - Concluded. Views of ice formations obtained at various icing and operating conditions with unheated blades.

Page intentionally left blank

Page intentionally left blank

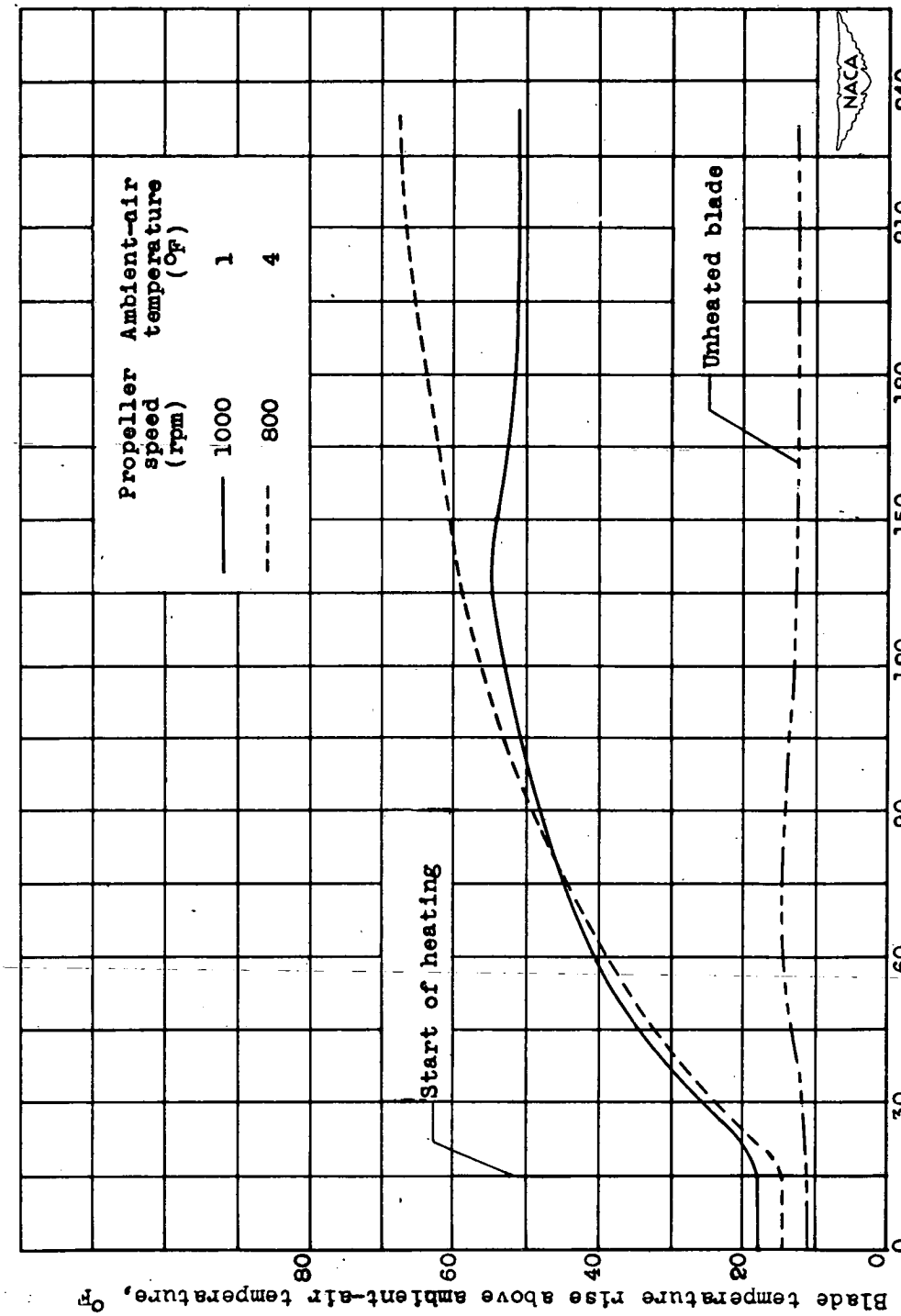

(a) Temperature rise of leading edge at 33-percent radius.

Figure 7.- Typical rise of blade-surface temperature above ambient-air temperature with continuous heating at power input of 1000 watts per blade.

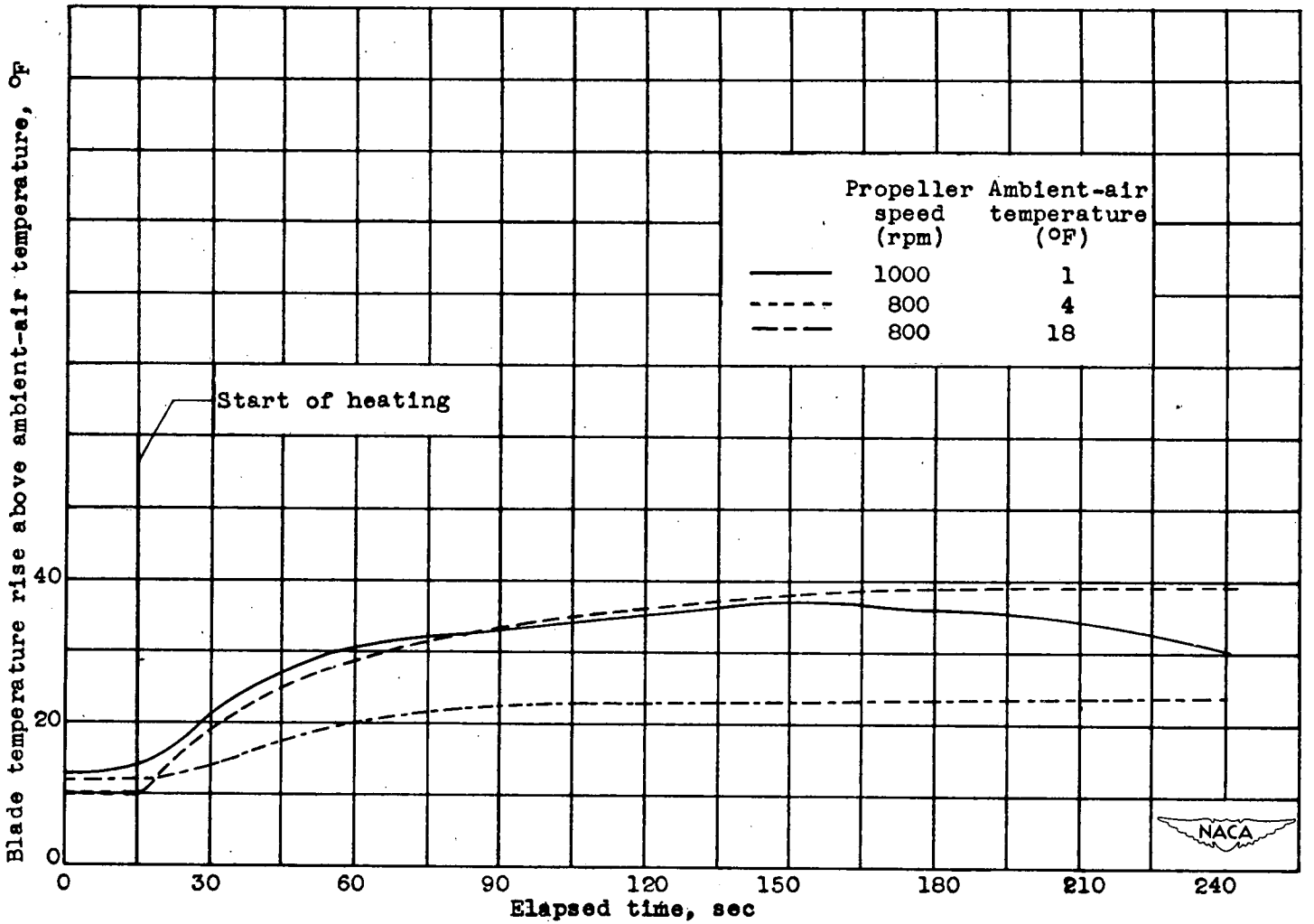

(b) Temperature rise 2 inches from leading edge on camber face at 33-percent radius.

Figure 7.- Concluded. Typical rise of blade-surface temperature above ambient-air temperature with continuous heating at power input of 1000 watts per blade.

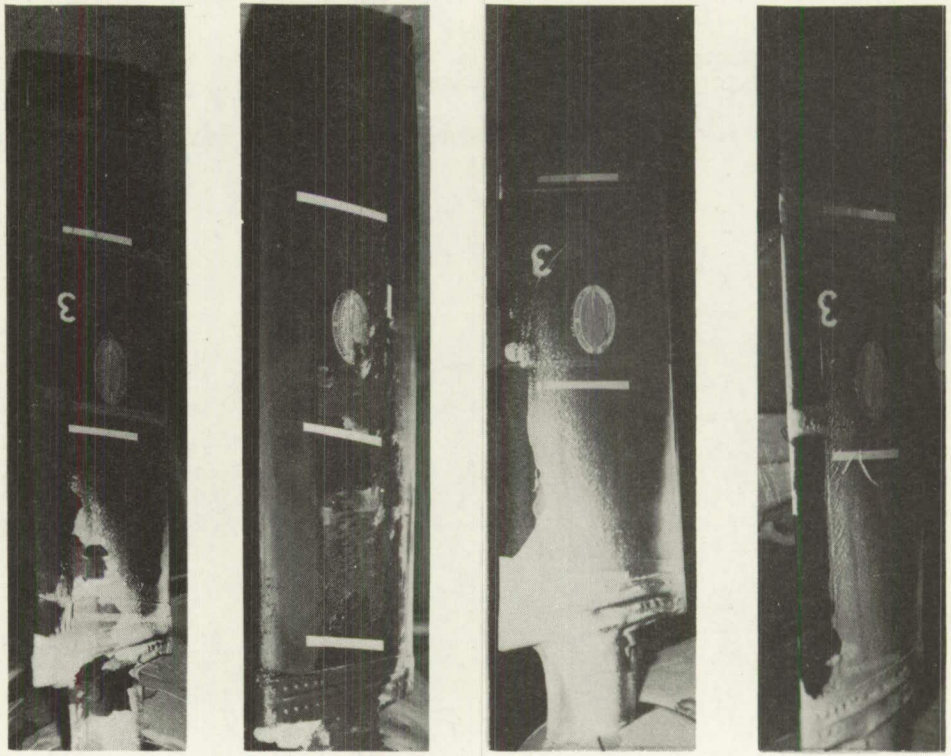

Condition (table 1)	D	C	E	F
Propeller speed, rpm	1000	800	800	800
Ambient-air temperature, °F	1	18	4	4
Liquid-water concentration, gram/cu m	0.2	0.7	0.2	0.2
Heat-on time, min	9	8	$3\frac{1}{2}$	6
Blade angle, deg	30.5	30.5	34.5	34.5
Power input, watts/blade	1000	1000	1000	1250

NACA C-20536 1-29-48

Figure 8. - Residual ice on camber face after continuous heating at several icing, heating, and operating conditions.

Page intentionally left blank

Page intentionally left blank

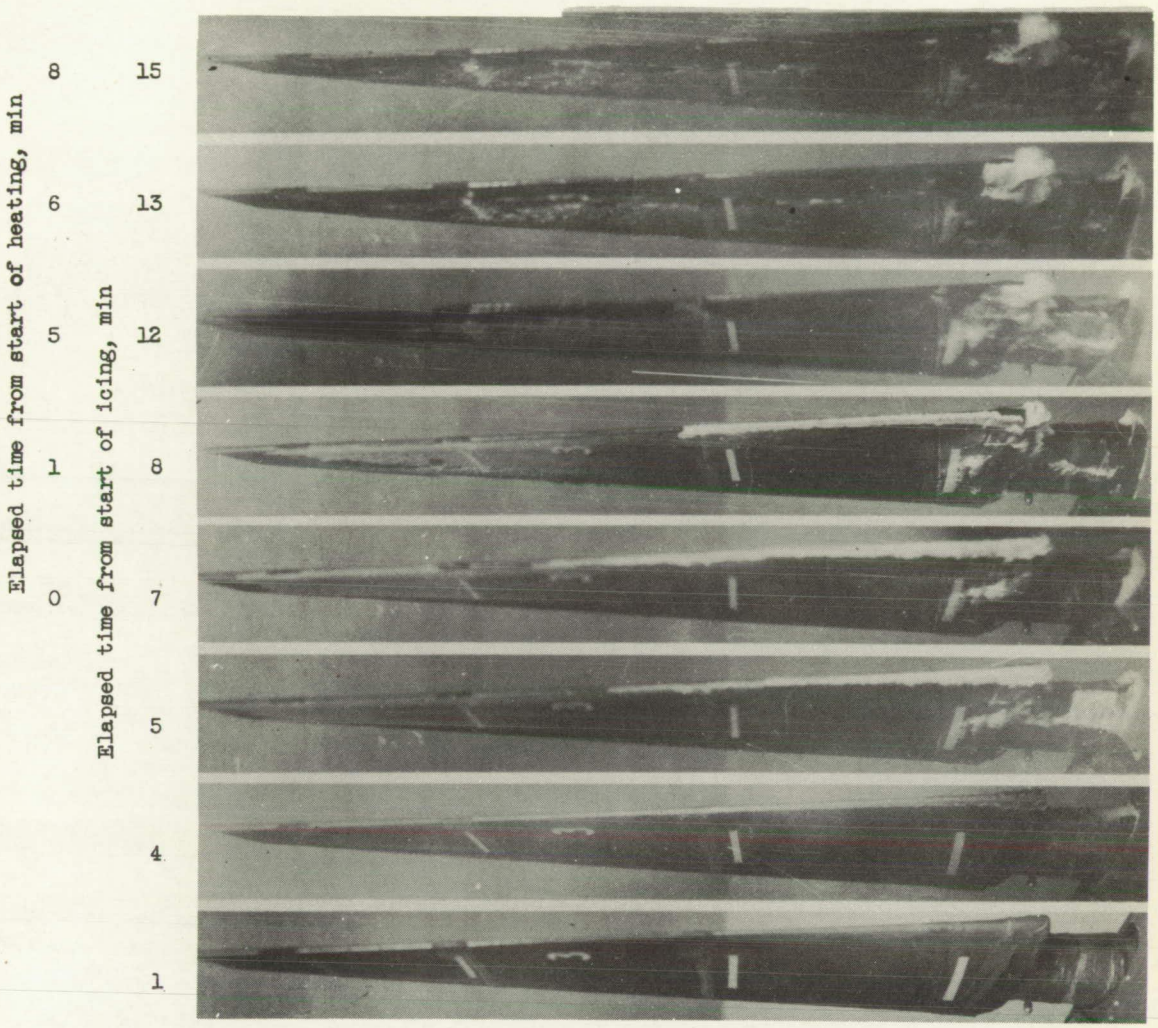

Figure 9. - Icing and de-icing of leading edge and thrust face with continuous heating. Condition C_o (table I): propeller speed, 800 rpm; ambient-air temperature, 18° F; blade angle, 30.5°; power input, 1000 watts per blade.

Page intentionally left blank

Page intentionally left blank

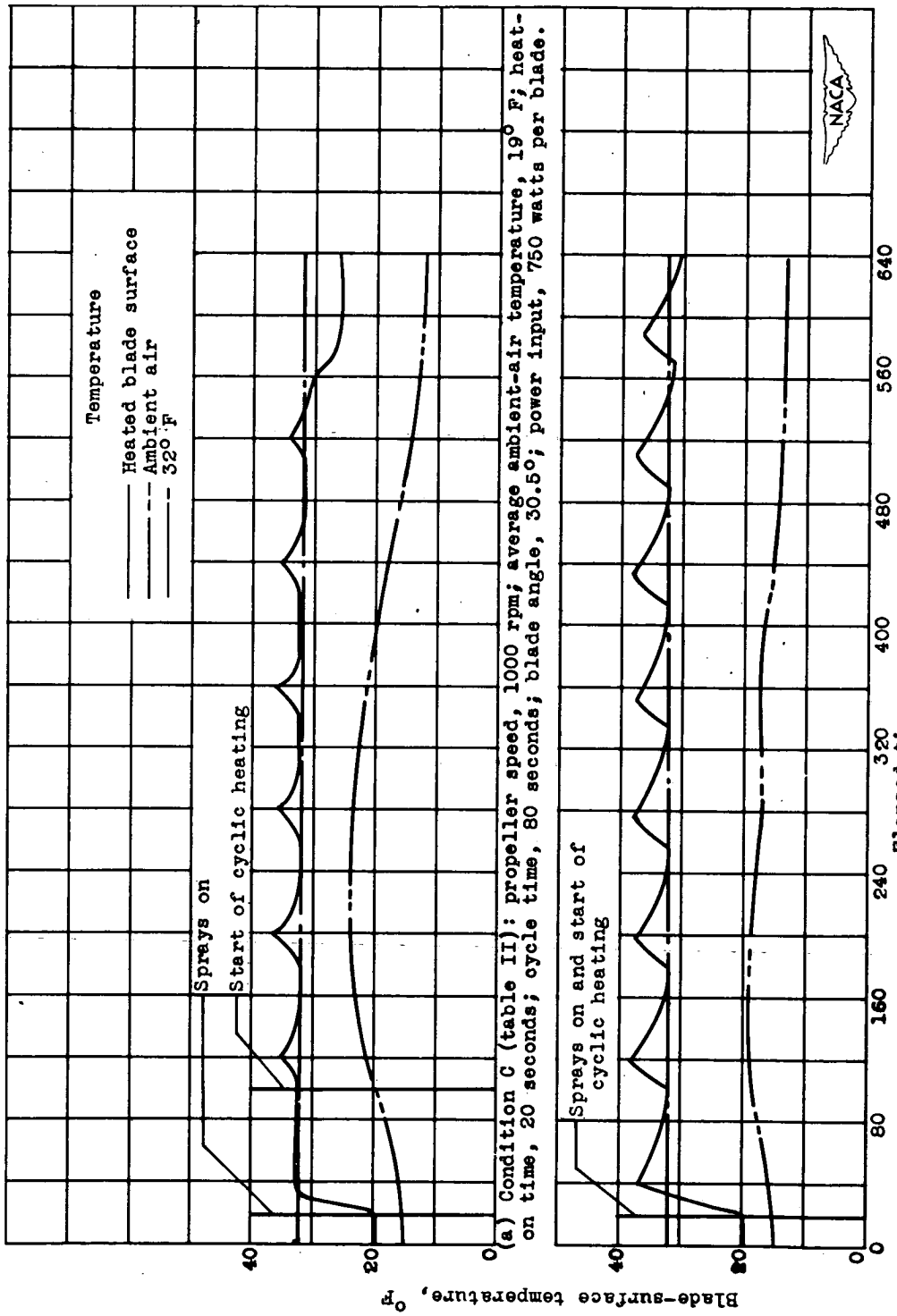

(a) Condition C (table II): propeller speed, 1000 rpm; average ambient-air temperature, 19° F; heat-on time, 20 seconds; cycle time, 80 seconds; blade angle, 30.5°; power input, 750 watts per blade.

(b) Condition M (table II): propeller speed, 800 rpm; average ambient-air temperature, 17° F; heat-on time, 20 seconds; cycle time, 80 seconds; blade angle, 34.5°; power input, 1000 watts per blade.

Figure 10. - Typical variation of leading-edge blade-surface temperature with time during cyclic deicing at 33-percent radius.

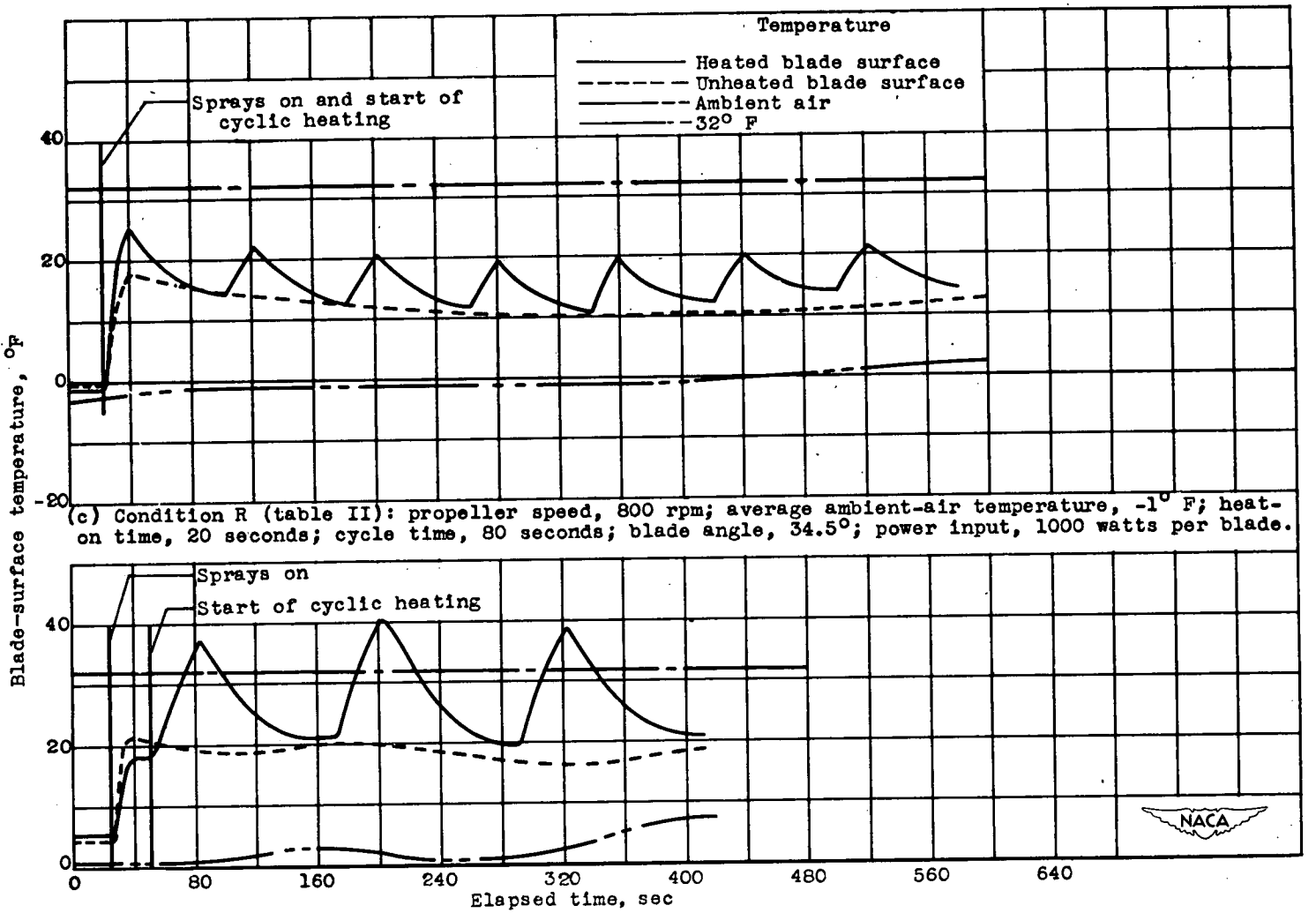

(c) Condition R (table II): propeller speed, 800 rpm; average ambient-air temperature, -1° F; heat-on time, 20 seconds; cycle time, 80 seconds; blade angle, 34.5°; power input, 1000 watts per blade.

(d) Condition S (table II): propeller speed, 800 rpm; average ambient-air temperature, 3° F; heat-on time, 32 seconds; cycle time, 120 seconds; blade angle, 34.5°; power input, 1000 watts per blade.

Figure 10. - Continued. Typical variation of leading-edge blade-surface temperature with time during cyclic de-icing at 33-percent radius.

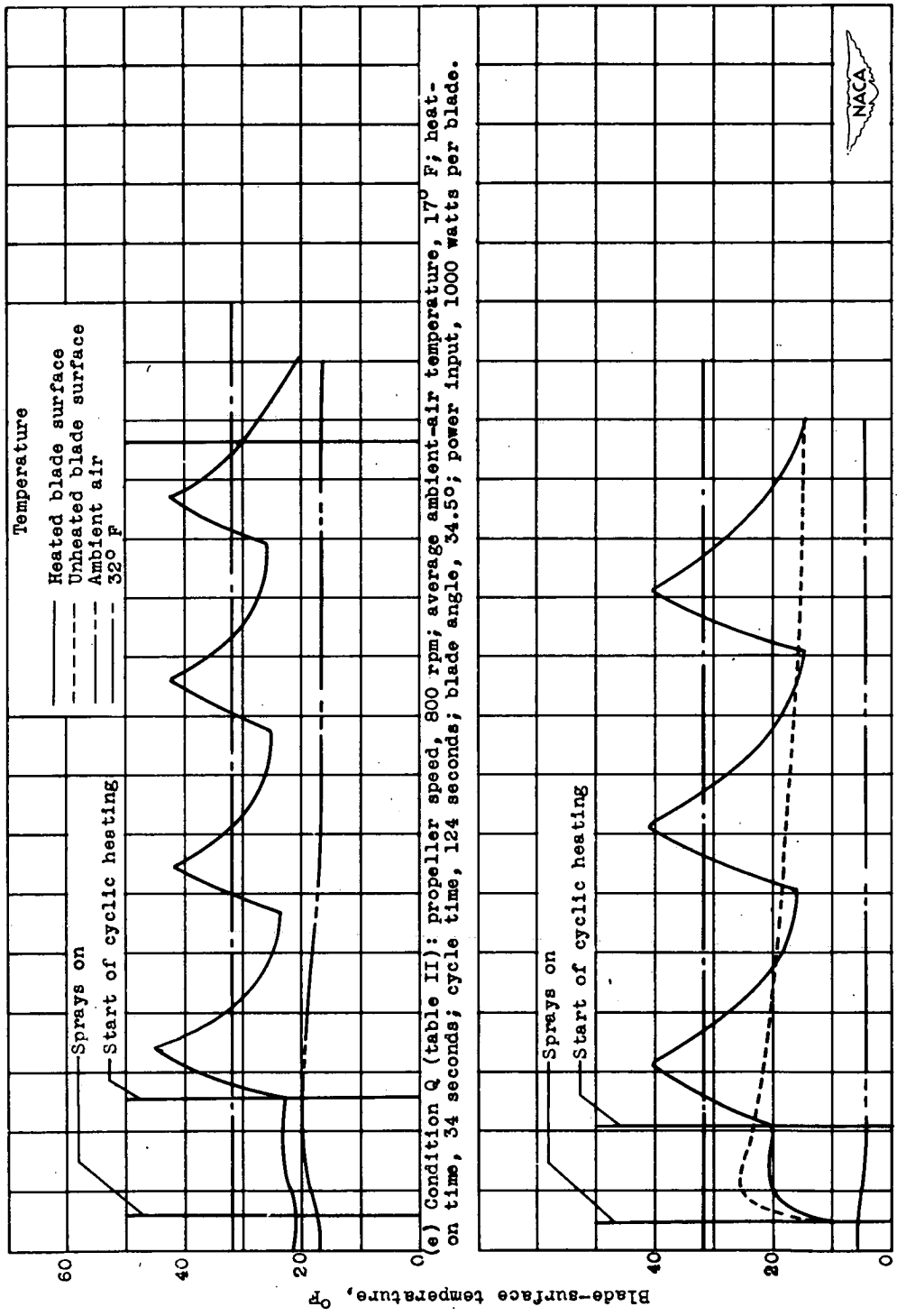

(e) Condition Q (table II): propeller speed, 800 rpm; average ambient-air temperature, 17° F; heat-on time, 34 seconds; cycle time, 124 seconds; blade angle, 34.5°; power input, 1000 watts per blade.

(f) Condition U (table II): propeller speed, 800 rpm; average ambient-air temperature, 5° F; heat-on time, 44 seconds; cycle time, 160 seconds; blade angle, 34.5°; power input, 1000 watts per blade.

Figure 10. - Continued. Typical variation of leading edge blade-surface temperature with time during cyclic de-icing at 35-percent radius.

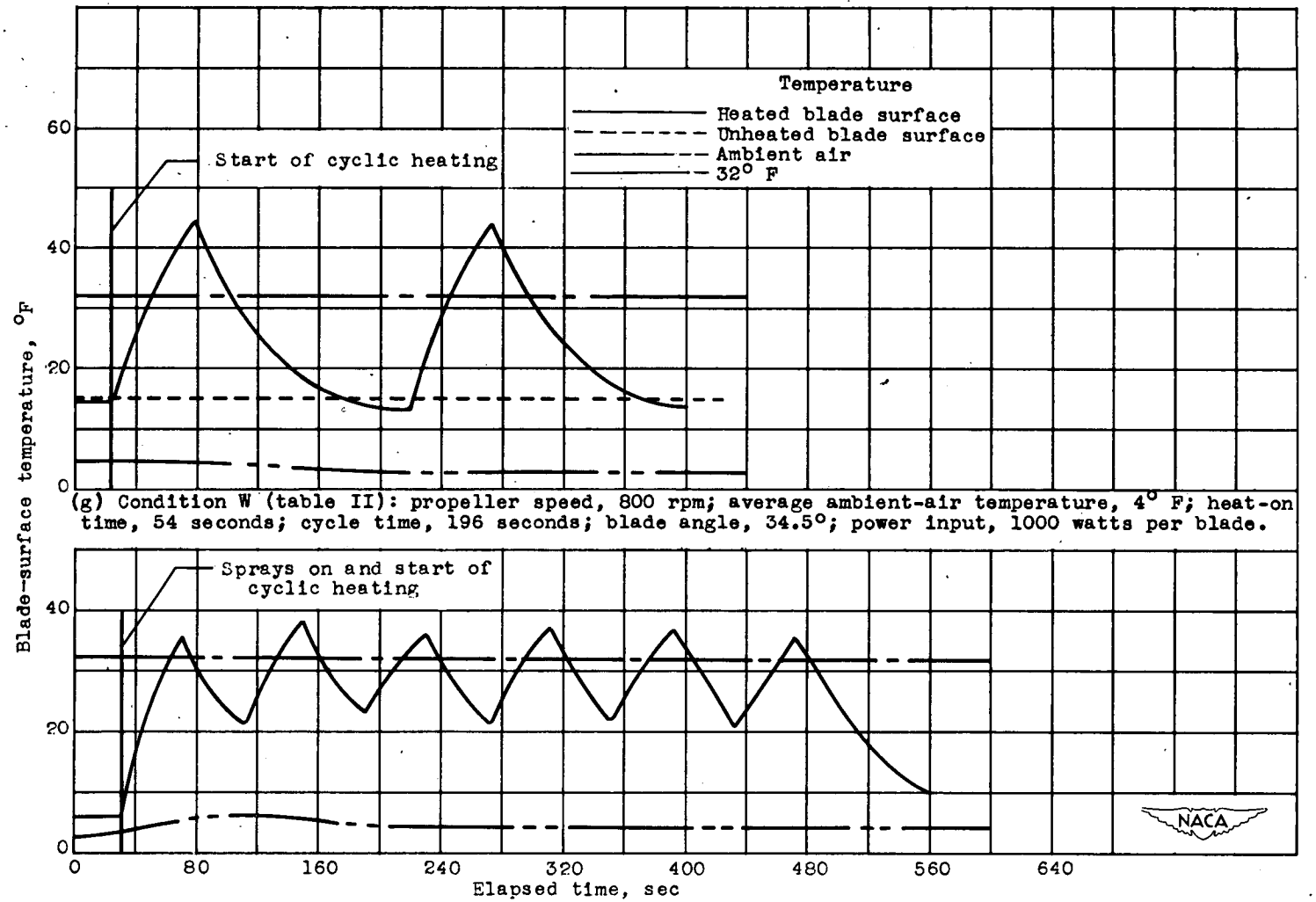

(g) Condition W (table II): propeller speed, 800 rpm; average ambient-air temperature, 4° F; heat-on time, 54 seconds; cycle time, 196 seconds; blade angle, 34.5°; power input, 1000 watts per blade.

(h) Condition V (table II): propeller speed, 800 rpm; average ambient-air temperature, 5° F; heat-on time, 40 seconds; cycle time, 80 seconds; blade angle, 34.5°; power input, 1250 watts per blade.

Figure 10. - Continued. Typical variation of leading edge blade-surface temperature with time during cyclic de-icing at 33-percent radius.

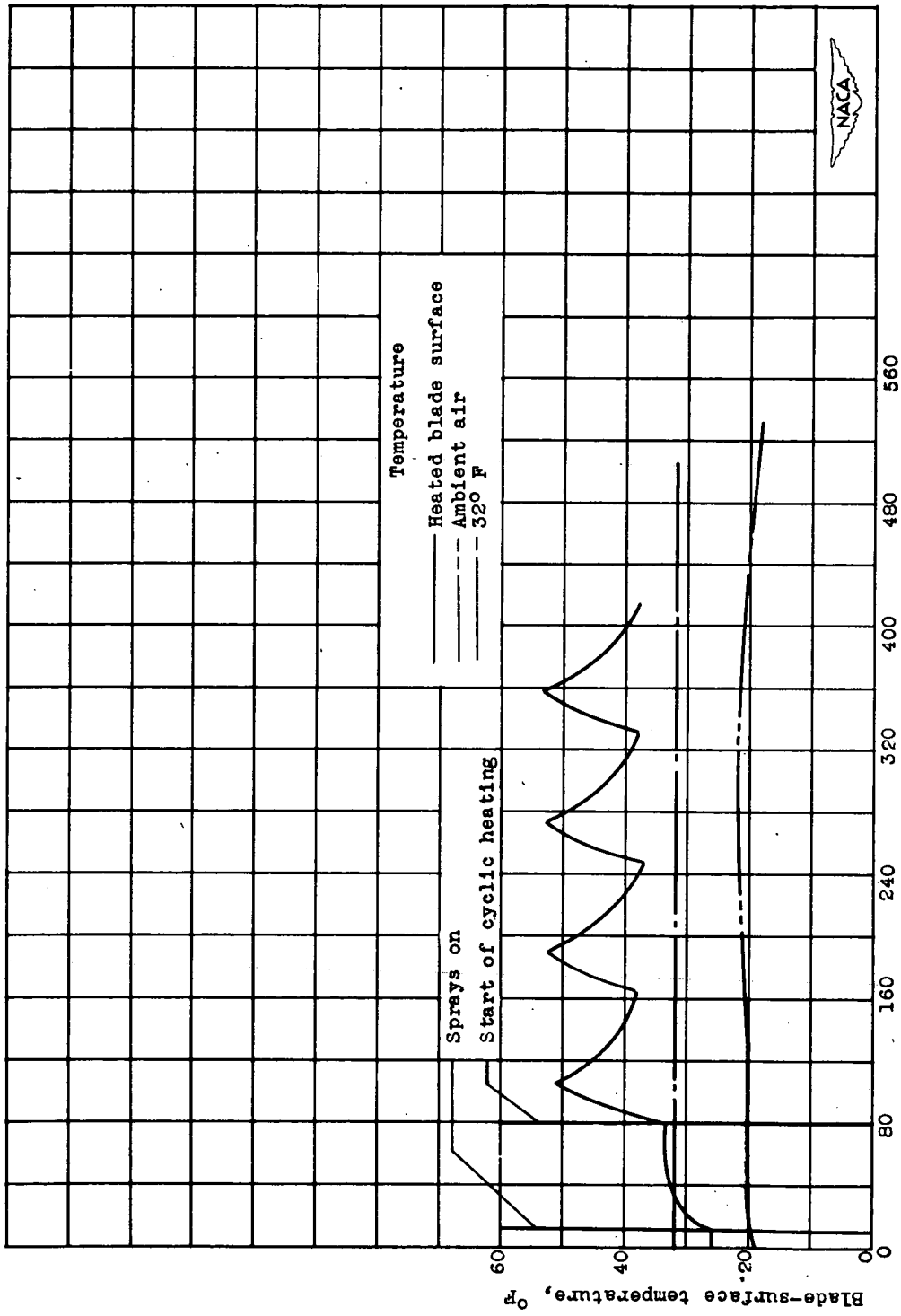

(1) Condition N (table II): propeller speed, 800 rpm; average ambient-air temperature, 20° F; heat-on time, 24 seconds; cycle time, 84 seconds; blade angle, 34.5°; power input, 1250 watts per blade.

Figure 10. - Concluded. Typical variation of leading-edge blade-surface temperature with time during cyclic de-icing at 35-percent radius.

Page intentionally left blank

Page intentionally left blank

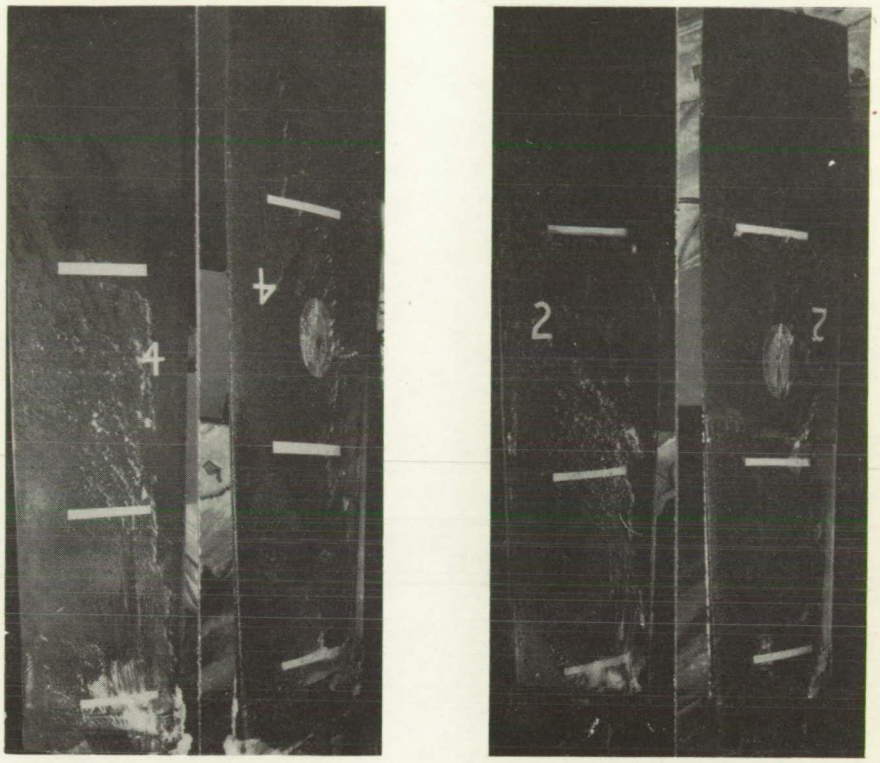

	Thrust Camber	Thrust Camber
Condition (table II)	P	0
Ambient-air temperature, °F	21	20
Liquid-water concentration, gram/cu m	0.9	0.8
Cycle time, sec	120	240

NACA
C-20537
1-29-48

(a) Propeller speed, 800 rpm; heat-on time, 30 seconds; blade angle, 34.5°; power input, 750 watts per blade.

Figure 11. - Residual ice after cyclic de-icing.

Page intentionally left blank

Page intentionally left blank

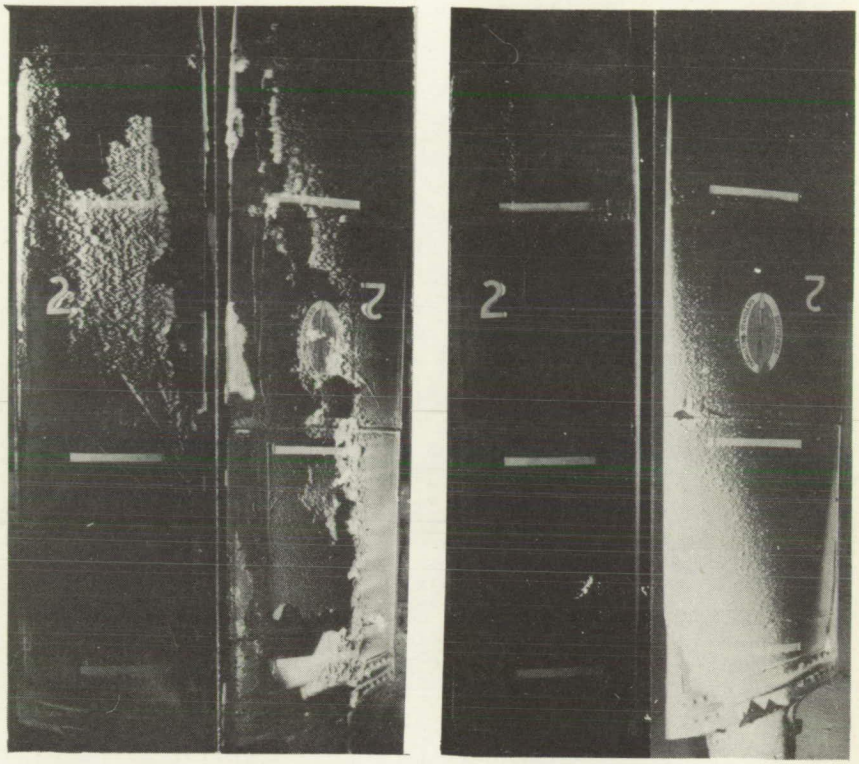

	Thrust Camber	Thrust Camber
Condition (table II)	M	R
Ambient-air temperature, ^{o}F	17	-1
Liquid-water concentration, gram/cu m	0.7	0.3

NACA
C-20538
1-29-48

(b) Propeller speed, 800 rpm; heat-on time, 20 seconds; cycle time, 80 seconds; blade angle, 34.5°; power input, 1000 watts per blade.

Figure 11. - Continued. Residual ice after cyclic de-icing.

Page intentionally left blank

Page intentionally left blank

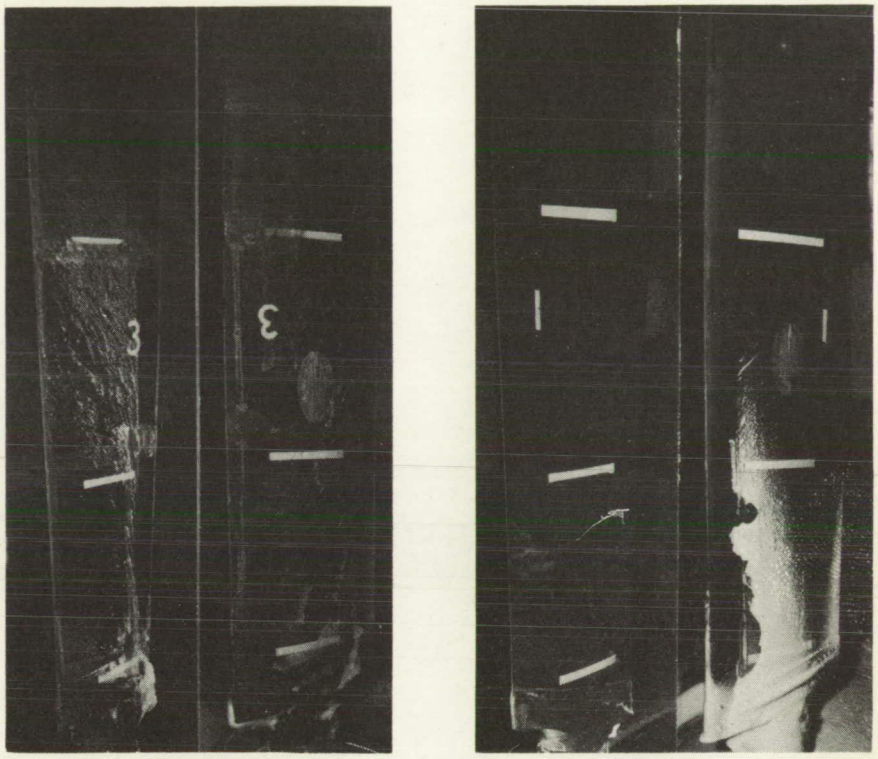

	Thrust Camber	Thrust Camber
Condition (table II)	N	V
Ambient-air temperature, ^{o}F	20	5
Liquid-water concentration, gram/cu m	0.8	0.3
Heat-on time, sec	24	40
Cycle time, sec	84	80

NACA
C-20539
1-29-48

(c) Propeller speed, 800 rpm; blade angle, 34.5°; power input, 1250 watts per blade.

Figure 11. - Continued. Residual ice after cyclic de-icing.

Page intentionally left blank

Page intentionally left blank

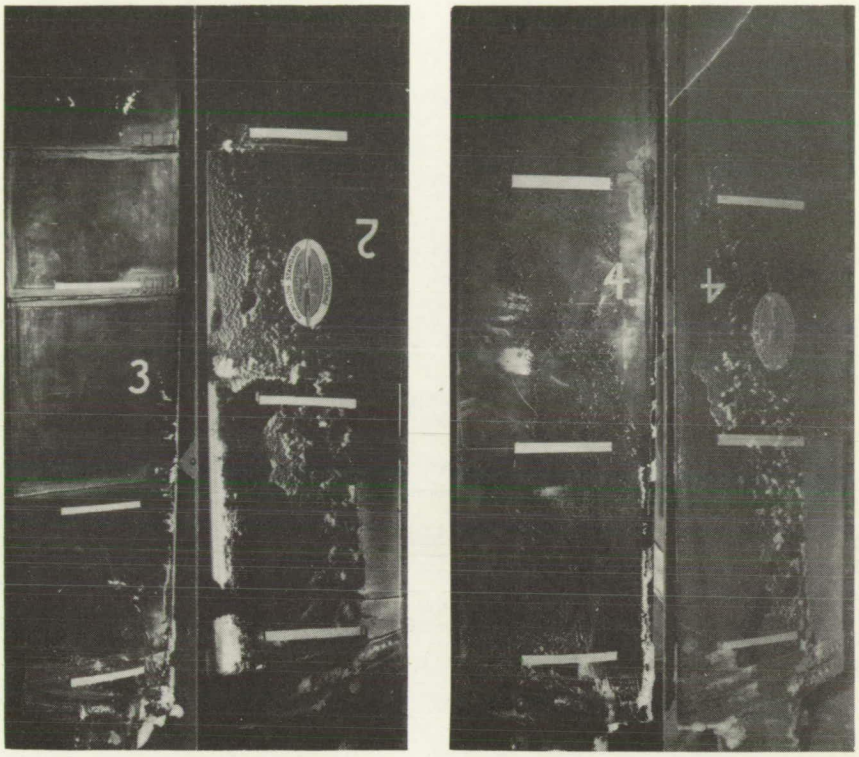

	Thrust Camber	Thrust Camber
Condition (table II)	H	G
Ambient-air temperature, °F	17	20
Liquid-water concentration, gram/cu m	0.7	0.8
Cycle time, sec	80	160

NACA
C-20540
1-29-48

(d) Propeller speed, 1000 rpm; heat-on time, 20 seconds; blade angle, 30.5°; power input, 750 watts per blade.

Figure 11. - Continued. Residual ice after cyclic de-icing.

Page intentionally left blank

Page intentionally left blank

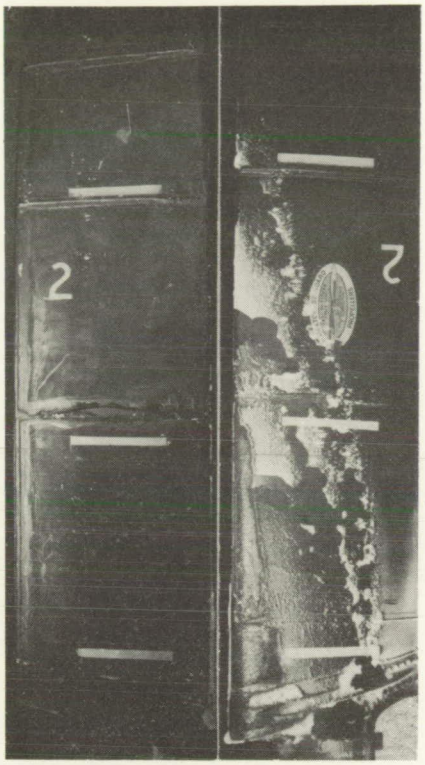

Thrust Camber

Thrust Camber

Condition (table II)	B	I
Ambient-air temperature, ^{o}F	17	18
Liquid-water concentration, gram/cu m	0.7	0.7
Heat-on time, sec	5	20
Cycle time, sec	20	80

NACA
C-20541
1-29-48

(e) Propeller speed, 1000 rpm; blade angle, 30.5°; power input, 1000 watts per blade.

Figure 11. - Concluded. Residual ice after cyclic de-icing.

Page intentionally left blank

Page intentionally left blank

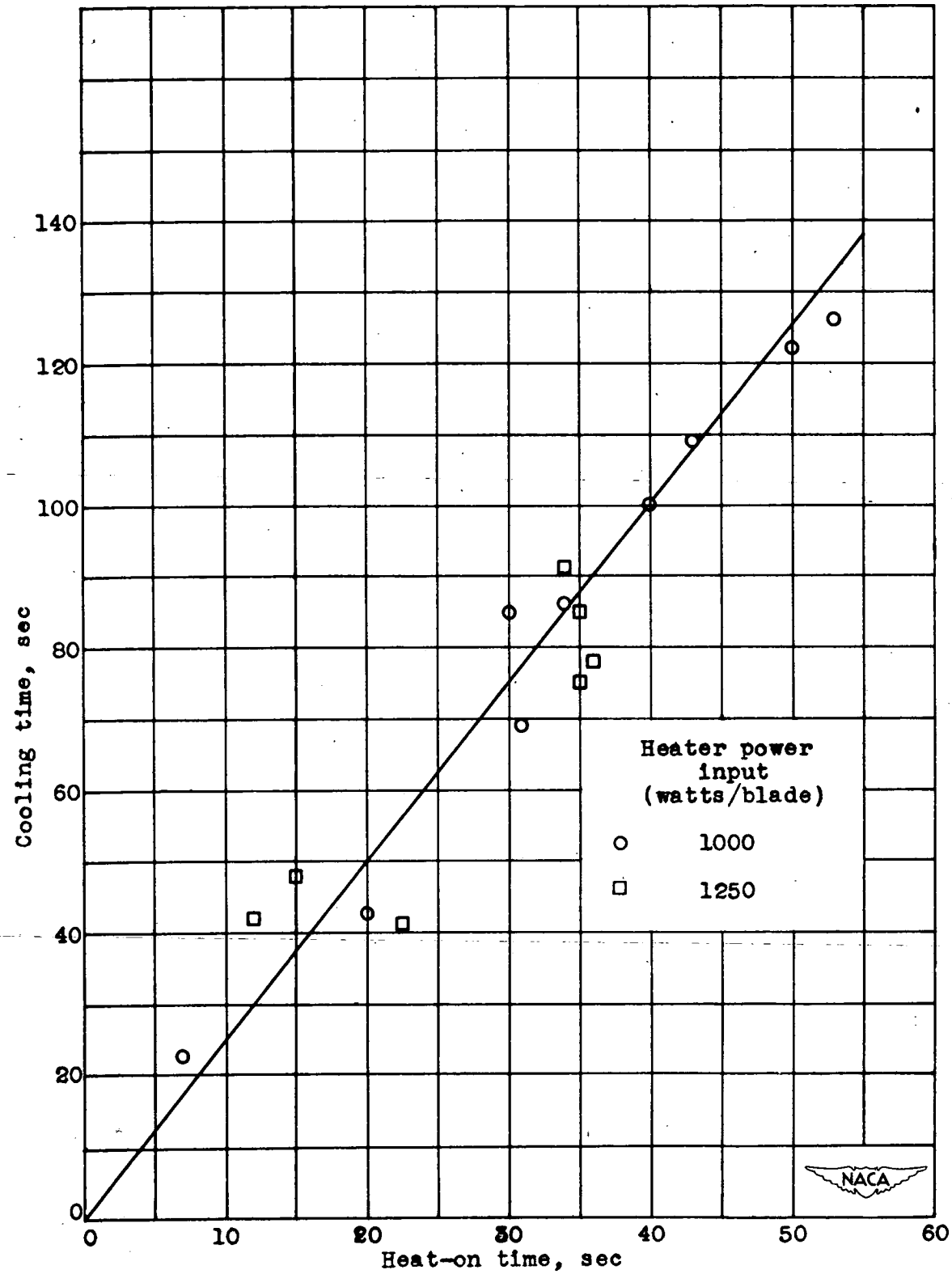

Figure 12.- Variation of optimum cooling time with heat-on time.